Electron localization effects on the conducting state in polyaniline

1994 J. Phys.: Condens. Matter 6 5631

(http://iopscience.iop.org/0953-8984/6/29/005)

J. Phys.: Condens. Matter 6 (1994) 5631–5638. Printed in the UK

Electron localization effects on the conducting state in polyaniline

P K Kahol†‡, N J Pinto†, E J Berndtsson† and B J McCormick§

† Department of Physics, Wichita State University, Wichita, KS 67208, USA
‡ National Institute for Aviation Research, Wichita State University, Wichita, KS 67208, USA
§ Department of Chemistry, Wichita State University, Wichita, KS 67208, USA

Received 3 December 1993, in final form 5 April 1994

Abstract. Electron localization effects in polyaniline have been investigated through the dependence of DC conductivity and magnetic susceptibility on thermal aging. A dramatic effect of thermal aging on conductivity is reported in the insulator-to-metal transition region, which is interpreted as due to the onset of structural order between the chains. This is argued to confirm that the insulator-to-metal transition corresponds to a crossover of the electron states from localization to delocalization. Furthermore, the quasi-one-dimensional variable-range hopping model is shown to account for the observed temperature dependences of the conductivity in the entire protonation range.

1. Introduction

Conjugated polymers have recently emerged as materials of tremendous importance for applied and basic research [1]. In particular, polyaniline (PAN) protonated with HCl (PAN-Cl) displays a rich variety of complex but novel physics. While it is well established that PAN-Cl exhibits an insulator-to-metal transition determined by the protonation level $y = [Cl^-]/[N]$, the nature of charge transport and the dimensionality of the metallic state have remained the subjects of recent study [2–8]. From the nearly linear dependence [9] of Pauli susceptibility (χ_P) on y and that of thermoelectric power on inverse temperature [4, 5], it seems clear that polyaniline in the emeraldine-salt-form phase segregates into either granular three-dimensional metallic islands surrounded by amorphous regions [2, 4, 5, 9] or isolated conducting chains in an insulating matrix [3]. In the metallic-island model, PAN-Cl (for y values in the range 0.3–0.5) is described as bundles of coupled parallel chains in which the electronic wave functions are completely delocalized over the entire bundle. The metallic bundles are associated with the 'crystalline' regions of the polymer, and interbundle barriers [10] determine macroscopic DC conductivity (σ). The same picture obtains for the isolated-conducting-chain case except that weak interchain interactions among the isolated chains limit the conductivity to modest values of the order of 10 Ω^{-1} cm^{-1}. Experimentally, however, it is observed that the conductivity changes over nine orders of magnitude in the protonation range $0.2 < y < 0.3$ [11]. In the three-dimensional metallic-islands picture, this insulator-to-metal transition represents a crossover from localization to delocalization of electronic states within the islands, whereas, in the conducting-chains model, the transition arises from percolation of isolated protonated chains [12]. The insulator-to-metal transition is also described in other studies as due to disorder in the sequence of benzenoid and

0953-8984/94/295631+08$19.50

quinoid groups along the polymer chain [7], and due to the presence of extended states in the random dimer model [6, 8].

The purpose of this paper is to show that the insulator-to-metal transition in PAN-Cl is driven by disorder and that it essentially represents a crossover from localization to delocalization brought about by increased structural order (and decreased separation) between protonated chains. The primary impetus for conducting this research comes from our prior magnetic susceptibility studies, which showed an unambiguous dependence of Curie and Pauli susceptibilities on absorbed moisture [13–15]. The presence of water, possibly associated with solvation of dopant ions such as chloride (due to its high charge-to-radius ratio in this case), is believed to reduce electrostatic Coulomb interaction between the positive charge on the chain and the anions, and thus increase delocalization of the spins on the polymer backbone. Removal of water through thermal aging, on the other hand, leads to decreased delocalization of the spins due to enhanced pinning of both the spin and the charge on the polymer chains. We report and discuss here the rather dramatic effect of aging on σ, which manifests itself in two distinctly different ways across the insulator–to–metal transition region. Furthermore, using the hopping-transport model for a weakly disordered quasi-one-dimensional (1D) system, [16, 17] it is shown that delocalization of the electron wave function occurs in the metal–to–insulator transition region.

Recent studies of PAN protonated with camphor sulphonic axis (PAN-CSA) have also shown that the insulator-to-metal transition is induced by disorder, and the polymer can be tuned through the critical regime of the metal-insulator by either pressure or external magnetic field [18-20]. The difference in the electrical and magnetic behaviour between PAN-Cl and PAN-CSA is due to reduced microscopic disorder and mesoscale inhomogeneities in PAN-CSA compared to PAN-Cl. Reduced microscopic disorder in PAN-CSA leads to intrinsically metallic states for $T \gtrsim 180$ K, whereas in PAN-Cl the conduction is of hopping type in the entire temperature regime 10–300 K with disorder-induced localization of the electron states.

2. Experimental details

The polyaniline samples were synthesized by the usual method as described earlier [21]. For σ measurements pellets were pressed under a pressure of approximately 10 kbar. A four-probe technique was used for conductivity measurements, with the four probes attached to the samples with Acheson Electrodag 502. A Keithley 614 electrometer was used to measure the voltage, while a Keithley 220 current source provided the electric current. Susceptibility measurements were made with a 'force' magnetometer in a magnetic field of 5 kG. Thermal aging of the samples was carried out in a vacuum of about 50×10^{-3} Torr, and the samples, once loaded, were not exposed to the external environment.

3. Results and discussion

Figure 1 shows the temperature dependence of DC conductivity, plotted as $\ln\sigma$ against $T^{-1/2}$, for the heavily doped sample of PAN-Cl ($y \simeq 0.52$) at different thermal aging temperatures. Two features of this set of curves are noteworthy. First, aging at higher temperatures leads not only to reduced room-temperature conductivity, but it also makes the temperature

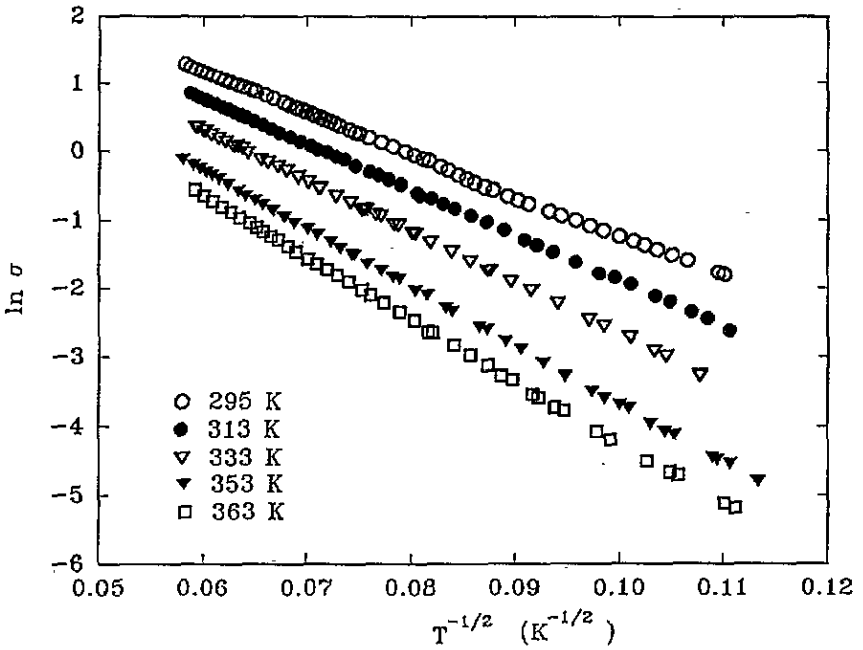

Figure 1. The temperature dependence of the DC conductivity of polyaniline doped at $y = 0.52 \pm 0.03$, plotted as $\ln(\sigma)$ against $T^{1/2}$, at different thermal aging temperatures: unaged sample (open circles); samples aged at 313 K (closed circles), 333 K (open triangles), 353 K (closed triangles), and 363 K (open squares).

dependence increasingly steep. Second, samples aged at various temperatures show a linear behaviour of $\ln\sigma$ against $T^{-1/2}$ described by

$$\sigma = \sigma_0' \exp[-(T_0'/T)^{1/2}] \tag{1}$$

with nearly the same intercept on the $\ln\sigma$ axis. Similar trends are observed for samples protonated up to $y \simeq 0.25$. For $y \lesssim 0.25$, aging leads to a progressive increase of conductivity at room temperature, and the slope of the $\ln\sigma$ against $T^{-1/2}$ curves decreases, in contrast to the behaviour for $y \gtrsim 0.25$ described above. A representative set of curves is shown in figure 2 at $y \simeq 0.14$. Furthermore, the conductivity as a function of temperature follows (1), at least up to $y \simeq 0.14$, below which it is represented by the following equation:

$$\sigma = (\sigma_0^*/T^{1/2}) \exp[-(T_0^*/T)^{1/4}]. \tag{2}$$

Figure 3 shows our results for $\ln(T^{1/2}\sigma)$ against $T^{-1/4}$ at $y = 0.10 \pm 0.02$. It should be noted that the data below $y \simeq 0.14$ cannot be represented by (1) [2].

The behaviour shown in figures 1–3 is considered to arise from an interplay between intrachain electronic disorder and interchain structural disorder. According to recent x-ray investigations, [10] crystallinity in PAN increases with increase in y, but even at $y = 0.50$, approximately half of the material is amorphous. Chains in the emeraldine-base form are inherently disordered—much like spaghetti—and protonation with concomitant incorporation of Cl^- anions between chains provides the necessary electrostatic forces for transforming a disordered structure into a compact 'ordered' structure, as shown by

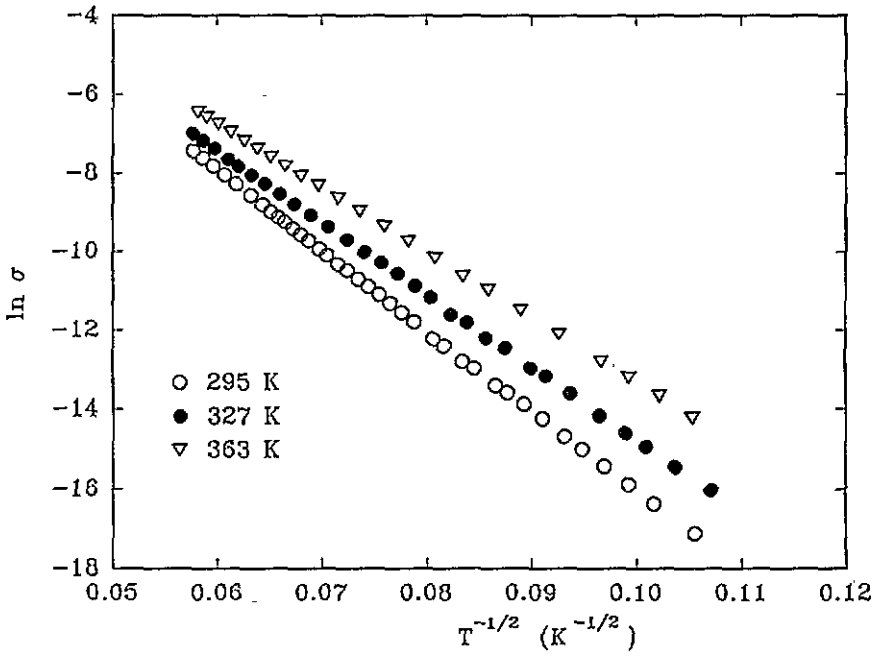

Figure 2. *The temperature dependence of the* DC *conductivity of polyaniline doped at* $y = 0.14 \pm 0.02$, plotted as $\ln(\sigma)$ against $T^{1/2}$, at different thermal aging temperatures: unaged sample (open circles); samples aged at 327 K (closed circles) and 363 K (open triangles).

a decrease in the d spacings between the chains with increase of y up to a limiting value y_c [10]. We argue that the interchain structural disorder for $y < y_c$, arising from the overwhelming amorphous content and small size of the semicrystalline regions, induces enough intrachain electronic disorder in this protonation range that the electron wave functions are localized on individual chains. Thermal aging for samples having $y < y_c$ reduces the interchain disorder of the loosely packed structure by introducing more regularity between the chains, leading thereby to increased localization length or decreased values of T_0'. This interpretation is supported by the recent x-ray diffraction results on an annealed sample of polyaniline doped with *p*-toluenesulphonic acid [22].

Above y_c, the crystalline regions are tightly packed, and we contend that water molecules hydrating the Cl^- anions contribute to the overall structural order of PAN-Cl [23]. Liberation of water by thermal aging introduces more intrachain electronic disorder through changes, for example, in the potential barriers at sites close to the Cl^- anions. This is reflected by a decrease in the localization length. The same effect is observed in other heavily doped derivatives of polyaniline, namely poly(*o*-toluidine), poly(*m*-toluidine), poly(*o*-ethyl aniline) and poly(*o*-propyl aniline), where random location of the long alkyl groups at two equivalent positions causes so much intrachain electronic disorder that the electron wave function is always localized on individual chains and thermal annealing does not lead to any significant additional localization [24]. What emerges therefore is the result that structural disorder in polyaniline localizes the charge to single chains for samples having $y < y_c$, and that the increased interchain structural order or coherence in the crystalline regions for $y > y_c$ leads to the appearance of delocalized electron states.

The results shown in figures 1–3 (in fact over the entire protonation range) can be quantitatively interpreted using a model that incorporates quasi-1D variable-range hopping

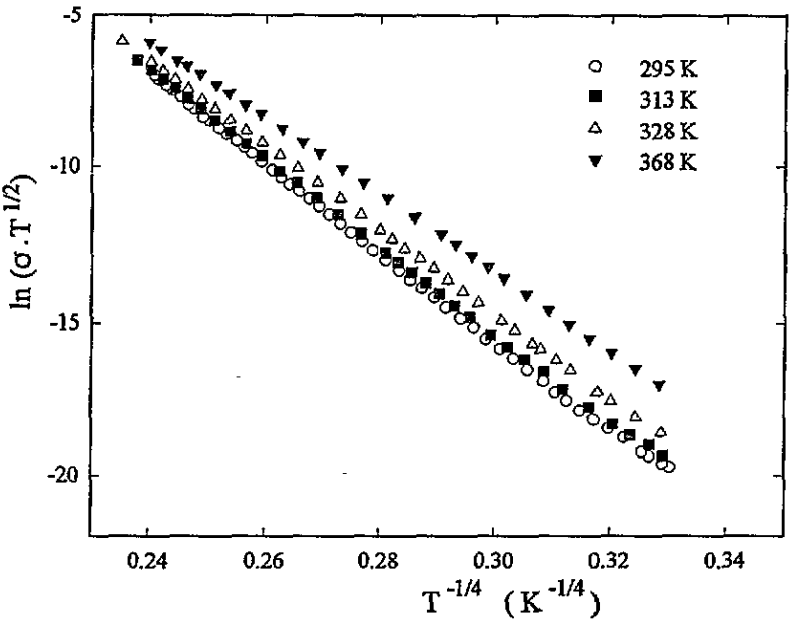

Figure 3. The temperature dependence of the DC conductivity of polyaniline doped at $y = 0.10 \pm 0.02$, plotted as $\ln(\sigma T^{1/2})$ against $T^{1/4}$, at different thermal aging temperatures: unaged sample (open circles); samples aged at 313 K (filled squares), 328 K (open triangles), and 368 K (filled triangles).

(VRH) between nearest-neighbouring chains [16, 17]. In such a quasi-1D system, consisting of N parallel chains with weak interchain interactions ($t_\perp \tau_i \ll \hbar$), conductivity is determined by three parameters, namely the temperature T_0, the density of states at the Fermi level $N(E_F)$, and the transfer integral $t_\perp$, which denotes interchain exchange between nearest-neighbour chains. T_0 is the characteristic temperature, above which conductivity is essentially determined by the phonon bath, and below which it is determined by the distributional disorder of electron states in space and energy. In the temperature range $T_1 < T < T_0$, where $T_1 = 3T_0/4\kappa$ with $\kappa = \ln(4T_0/\pi t_\perp)$ and $T_0 = T_0'/2$, interchain conductivity perpendicular to the chains is of the type $\ln\sigma \propto -(T_0'/T)^{1/2}$, and the intrachain conductivity is of the activated type. Interchain conductivity due to quasi-1D VRH retains the temperature dependence of equation (1) for the temperature range $T_2 < T < T_1$, where $T_2 = T_0/2\kappa^2$. The conductivity for $T < T_2/9$, however, corresponds to VRH in a 3D anisotropic system where $T_0^* = 512T_0\kappa^2$.

As long as σ follows (1) (figures 1 and 2), the slope of $\ln\sigma$ against $1/T^{1/2}$ yields T_0 directly, and thus the localization length can be obtained using the relationship $T_0 = 8/\alpha^{-1}N(E_F)zk_B$. Magnetic-susceptibility measurements were made under the same thermal aging conditions as the conductivity measurements to determine $N(E_F)$. Table 1 lists values of T_0, $N(E_F)$, and α^{-1} for the three reported samples. It is clear that thermal aging introduces intrachain disorder, which is then reflected in lower values of α^{-1}. However, for $y \lesssim 0.10$ (figure 3, for example) the measured slope gives T_0^*, which is proportional to $T_0\kappa^2$. An estimate of the hopping integral is needed to obtain T_0 as κ depends on both T_0 and $t_\perp$. Since the experimental data of figure 3 follow equation (2) from around 250 K downwards, we take $T_2 = 2000$ K, and making use of the relations $512T_0\kappa^2 = T_0^*$, $T_2 = T_0/2\kappa^2$,

Table 1. *The protonation level, thermal aging temperature, T_0, density of states at the Fermi level, and the localization length for the three polyaniline samples.*

Protonation level, y	Thermal aging temperature (K)	T_0 (K)	$N(E_F)$ (states eV^{-1}/2-ring)	α^{-1} (Å)
0.52 ± 0.03	295	1800	3.8	34
	313	2200	3.7	28
	333	2800	3.4	25
	353	3600	3.2	20
	365	4000	3.1	19
0.14 ± 0.02	297	20000	1.2	9
	327	165000	1.2	11
	363	135000	1.2	14
0.10 ± 0.02	295	52000	0.5	7
	313	50000	0.5	8
	328	46000	0.5	8
	368	40000	0.5	10

$\chi_P = \mu_B^2 N(E_F)$, and $T_0 = 8/\alpha^{-1} N(E_F) z k_B$, we find α^{-1} in the range 7–10 Å. For values of y lower than 0.10, we have used $T_2 = 3000$ K in the calculations for α^{-1} since (2) is followed beginning at room temperature. The plot in figure 4 of α^{-1} against y, especially for unaged samples of PAN-Cl, clearly shows delocalization of the electron spins in the transition region.

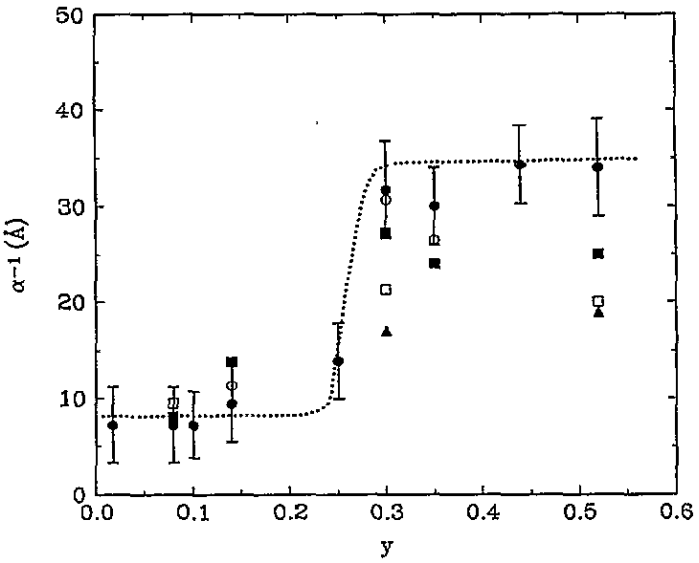

Figure 4. *The localization length α^{-1} as a function of protonation level y. The dotted line is a guide to the eye for results corresponding to the unaged samples (●). Various symbols for various y values correspond to the following aging temperatures: ○, 313 K; ■, 333 K; □, 353 K; ▲, 363 K for the $y = 0.52$ sample: ○, 323 K; ■, 363 K for the $y = 0.35$ sample; ○, 323 K; ■, 363 K; □, 388 K; ▲, 419 K for the $y = 0.30$ sample; ○, 327 K: ■, 363 K for the $y = 0.14$ sample; ○, 313 K; ■, 328 K; □, 368 K for the $y = 0.10$ sample. The same error bars as for the results on unaged samples apply to the results on aged samples.*

That the states in PAN-Cl are delocalized is also predicted by the above model. A localization to delocalization transition occurs when $J = 1$, where $J = (\pi^2/2^{1/2})(t_\perp/4T_0)$ and where $t_\perp$ can be approximately obtained from the relation $t_\perp = (2e^2/\epsilon a)(r/a)\exp(-r/a)$ [4]. Using $r = 3.5$ Å, $a = 1.06$ Å, $\epsilon = 4$, and experimentally determined values of T_0, we obtain $J = 3.2$, 2.4, 1.6, 0.7, and 0.3 corresponding to y values of 0.52, 0.44, 0.35, 0.25, and 0.14, respectively. This behaviour, that of decreasing J values, is mainly due to increased localization of the electrons as a result of decreased interchain coherence. For heavily protonated poly(*o*-toluidine) and poly(*o*-ethylaniline), the J values are 0.4 and 0.1, respectively [24].

4. Conclusions

In conclusion, the insulator-to-metal transition in PAN-Cl is of localization-to-delocalization type, driven by increased structural order between the chains and through increased interchain coherence. The inherent disorder present in alkyl-substituted polyanilines keeps the electron states localized on individual chains. The quasi-1D VRH model accounts for all the observed conductivity features as a function of both temperature and protonation level for polyaniline and its derivatives. Finally, absorbed moisture makes the most significant contribution to the factors affecting the interchain hopping parameters involved in the conduction process.

Acknowledgments

Thanks are due to the National Science Foundation (grant No OSR-95523) and the Petroleum Research Fund (grant No 24728-B7) for financial support of this work.

References

[1] Kahol P K, Clark W G and Mehring M 1992 *Conjugated Conducting Polymers (Springer Series in Solid-State Sciences 102)* ed H Kiess p 217
[2] Zuo F, Angelopuolos M, MacDiarmid A G and Epstein A J 1987 *Phys. Rev.* B **36** 3475; 1989 *Phys. Rev.* B **39** 3570
[3] Mizoguchi K, Nechtschein M, Travers J-P and Menardo C 1989 *Phys. Rev. Lett.* **63** 66
[4] Wang Z H, Ray A, MacDiarmid A G and Epstein A J 1991 *Phys. Rev.* B **43** 4373
[5] Wang Z H, Scherr E M, MacDiarmid A G and Epstein A J 1992 *Phys. Rev.* B **45** 4190
[6] Li Q, Cruz L and Phillips P 1993 *Phys. Rev.* B **47** 1840
[7] Galvao D S, dos Santos D A, Laks B, de Melo C P and Caldas M J 1989 *Phys. Rev. Lett.* **63** 786
[8] Phillips P and Wu H-L 1991 *J. Non-Cryst Solids* **137 & 138** 927
[9] Ginder J M, Richter A F, MacDiarmid A G and Epstein A J 1987 *Solid State Commun.* **63** 97
[10] Pouget J P, Josefowicz M E, Epstein A J, Tang X and MacDiarmid A G 1991 *Macromolecules* **24** 779
[11] Angelopoulos M, Ray A, MacDiarmid A G and Epstein A J 1987 *Synth. Met.* **21** 21
[12] Epstein A J, MacDiarmid A G and Pouget J P 1990 *Phys. Rev. Lett.* **65** 664
Mizoguchi K, Nechtschein M and Travers J P 1990 *Phys. Rev. Lett.* **65** 665
[13] Kahol P K, Guan H and McCormick B J 1991 *Phys. Rev.* B **44** 10393
[14] Kahol P K and McCormick B J 1991 *J. Phys.: Condens. Matter* **3** 7963
[15] Kahol P K and McCormick B J 1993 *Phys. Rev.* B **47** 14588
[16] Nakhmedov E P, Prigodin V N and Samukhin A N 1989 *Sov. Phys.–Solid State* **31** 368
[17] Prigodin V N, Firsov Yu A and Weller W 1986 *Solid State Commun.* **59** 729

[18] Reghu M, Cao Y, Moses D and Heeger A J 1993 *Phys. Rev.* B 47 1758
[19] Yoon C O, Reghu M, Moses D, Heeger A J and Cao Y 1993 *Phys. Rev.* B 48 14 080
[20] Sariciftci N S, Heeger A J and Cao Y 1994 *Phys. Rev.* B 49 5988
[21] MacDiarmid A G, Chang J, Halpern M, Huang W, Mu S, Somasiri N, Wu W and Yangier S 1985 *Mol. Cryst. Liq. Cryst.* **121** 173
[22] Kobayashi A, Ishikawa H, Amano K, Satoh M and Hasegawa E 1993 *J. Appl. Phys.* 74 296
[23] Boyle A, Penneau J F, Genies E and Riekel C 1992 *J. Polym. Sci.* B 30 265
[24] Pinto N J, Kahol P K, McCormick B J, Dalal N S and Wan H 1994 *Phys. Rev.* B at press